Krajcin, I.; Söffker, D.: Diagnosis and control of 3D elastic mechanical structures. Proc. 12th SPIE Symposium on Smart Structures and Materials, March 6-10, 2005, San Diego, CA, USA.

Diagnosis and control of 3D elastic mechanical structures

Idriz Krajcin and Dirk Söffker

Engineering Faculty, Chair of Dynamics and Control,
University Duisburg-Essen, Duisburg, Germany

ABSTRACT

In this paper, a model-based approach for fault detection and vibration control of flexible structures is proposed and applied to 3D-structures. Faults like cracks or impacts acting on a flexible structure are considered as unknown inputs acting on the structure. The Proportional-Integral-Observer (PI-Observer) is used to estimate the system states as well as unknown inputs acting on a system. Also the effects of structural changes are understood as external effects (related to the unchanged structure) and are considered as fictitious external forces or moments. The paper deals with the design of the PI-Observer for practical applications when measurement noise and model uncertainties are present and shows its performance in experimental results. As examples, impacts acting upon a one side clamped elastic beam and on a thin plate structure are estimated using displacement or strain measurements. To control the vibration of the flexible plate, two piezoelectric patches bonded on the structure are used as actuators. The control algorithm introduced in this contribution contains a state feedback control and additionally a disturbance rejection. The disturbances are estimated using the PI-Observer. Experimental results show the performance and the robustness properties of the control strategy for the vibration control of a very thin plate.

Keywords: Model-based diagnosis, vibration control, disturbance rejection, Proportional-Integral-Observer

1. INTRODUCTION

Smart structures have been the focus of several scientific efforts in the last decade. Lightweight structures have the advantage of saving weight and space but structural vibrations are an inevitable result. Smart structures integrate sensors, actuators and algorithms for control and diagnosis to respond to the changing environment and to compensate faults within the structure. Different actuator types, such as based on piezoelectric materials, shape memory alloys, electrostrictive materials and magnetorheological fluids have been considered to design smart structures. Piezoelectric materials can readily be embedded in structures and be used as both actuators and sensors. They are currently the most popular and the most used material in smart structures. A review of the state of the art of smart structures and integrated systems is given in reference.[1]

The vibrations in elastic structures can yield to damages of the structure. In order to ensure safe operating conditions, it is necessary to detect and localize damages as they occur. For practical applications, smart structures should become intelligent structures with self-diagnosis properties. Various technologies for fault detection have been used over the last decade, usually signal-based or model-based. Signal based methods[2] do not need a model of the structure while model-based methods[3–5] need an analytical model of the structure or/and the fault in order to detect and localize or isolate a fault avoiding failures of the considered system.

In this contribution, the PI-Observer[4,6] is used to estimate the non-measured states as well as the unknown input forces acting on an elastic structure using a small number of measurements. The observer can be used to detect faults like impacts acting on the structure or for example any kind of changes of stiffness e.g. cracks or delamination which can be considered as equivalent to local virtual forces.[7] Here, the problem of detecting faults is reduced to the problem of estimating unknown forces acting on a structure. The estimated states can

Further author information:
I.K.: E-mail: krajcin@uni-duisburg.de, Telephone: +49 (0)203 3793023
D.S.: E-mail: soeffker@uni-duisburg.de, Telephone: +49 (0)203 3793429

be used for further diagnosis algorithms or for vibration control of the structures and the unknown inputs as disturbances can also be used for diagnosis and control. Experimental results estimating impact forces acting on a one side clamped elastic beam are already presented in reference.[4] Here, detailed analytical considerations for the design of the PI-Observer are given if measurement noise and system uncertainties are present. To localize an unknown external force, a concept using parallel PI-Observers is introduced in this paper for the first time. The PI-Observer can be applied to any 3D structure, if the model of the structure is known. Additionally, the observer is applied to a plate structure for the first time. The performance of the observer estimation of unknown external forces acting on an elastic beam and on an elastic plate structure is presented. The observer estimations are based on displacement and strain gage measurements.

The control approaches used in adaptive structures can be distinguished into active and passive ones. Passive control strategies[8] uses an external shunt circuit which works as electrical damper. Active-passive hybrid piezoelectric networks are introduced and compared in reference.[9] A common used active control approach is the proportional feedback of the strain and the derivative of the strain using collocated piezoelectric materials, one as sensor and one as actuator. An overview of control design methods in smart structures is given in references.[1,10] In this contribution, a state feedback control with an additional disturbance rejection control is introduced. The PI-Observer is used to estimate the states and the unknown disturbances. The control approach is robust against uncertainties of the actuator model and external disturbances. In contrast to other approaches, the proposed model-based approach uses only 1-2 piezoelectric patches as actuators to control the vibrations for a wide frequency range. Experimental results show the performance and the robustness properties of the control strategy for the vibration control of a very thin plate.

2. DESIGN OF A PROPORTIONAL-INTEGRAL-OBSERVER

Consider the time invariant system

$$\dot{x}(t) = Ax(t) + Bu(t) + Nn(t)\,, \tag{1}$$
$$y(t) = Cx(t)\,, \tag{2}$$

with the state vector $x(t)$ of order n_d, the measurement vector $y(t)$ of order r_1 and the input vector $u(t)$ of order m. The system matrix A, the input matrix B and the output matrix C are of appropriate dimensions. The vector $n(t)$ of order r_2 describes an unknown part of the system. For example, this could be a nonlinear part of the system or arbitrary unknown external forces acting on the system. The matrix N locates the unknown inputs to the system and is assumed to be known.

The states and the additive unknown inputs can be estimated by the PI-Observer[6,11,12]

$$\begin{bmatrix} \dot{\hat{x}}(t) \\ \dot{f}(t) \end{bmatrix} = \begin{bmatrix} A & N \\ 0 & 0 \end{bmatrix} \begin{bmatrix} \hat{x}(t) \\ f(t) \end{bmatrix} + \begin{bmatrix} B \\ 0 \end{bmatrix} u(t) + \begin{bmatrix} L_1 \\ L_2 \end{bmatrix} (y(t) - \hat{y}(t)), \tag{3}$$
$$\hat{y}(t) = \begin{bmatrix} C & 0 \end{bmatrix} \begin{bmatrix} \hat{x}(t) \\ f(t) \end{bmatrix}. \tag{4}$$

The model (1) is extended by the modeled disturbances $f(t) \approx n(t)$. Considering the estimation error as $e(t) = \hat{x}(t) - x(t)$, the error dynamics of (3)

$$\begin{bmatrix} \dot{e}(t) \\ \dot{f}(t) \end{bmatrix} = \begin{bmatrix} A - L_1C & N \\ -L_2C & 0 \end{bmatrix} \begin{bmatrix} e(t) \\ f(t) - n(t) \end{bmatrix}, \tag{5}$$

with $f_e(t) = f(t) - n(t)$ is derived to

$$\begin{bmatrix} \dot{e}(t) \\ \dot{f}_e(t) \end{bmatrix} = \begin{bmatrix} A - L_1C & N \\ -L_2C & 0 \end{bmatrix} \begin{bmatrix} e(t) \\ f_e(t) \end{bmatrix} - \begin{bmatrix} 0 \\ \dot{n}(t) \end{bmatrix}. \tag{6}$$

In frequency domain the estimation errors are described by

$$e(s) = [Is - (A - L_1 C)]^{-1} N f_e(s) \,, \tag{7}$$
$$f_e(s) = -[Is - L_2 C(Is - (A - L_1 C))^{-1} N]^{-1} s\, n(s) \,. \tag{8}$$

Considering the extended system Eq. (3) described by the extended matrices

$$A_e = \begin{bmatrix} A & N \\ 0 & 0 \end{bmatrix} \quad \text{and} \quad C_e = \begin{bmatrix} C & 0 \end{bmatrix}, \tag{9}$$

the system is assumed to be observable if

$$\operatorname{rank} \begin{bmatrix} \lambda I_{n_d} - A & -N \\ 0 & \lambda I_{r_2} \\ C & 0 \end{bmatrix} = n_d + r_2 \tag{10}$$

holds. From Eq. (6) it can be seen that the derivation of the unknown inputs acts on the error equation. The requirement of successful estimation yields to decoupling or minimization of the transfer function from $\dot{n}(t)$ to the extended states $f_e(t)$ and the states $e(t)$. There are many different design techniques for the calculation of the feedback matrices. Here, the Loop Transfer Recovery (LTR) design method[11, 13] is applied to design the observer feedback matrices. The feedback matrix L is calculated solving the Riccati equation

$$A_e P + P A_e^T + Q - P C_e^T R^{-1} C_e P = 0 \,, \quad L = P C_e^T R^{-1} \,. \tag{11}$$

In the LTR design, the matrix M defined by

$$M = [Is - (A_e - L C_e)]^{-1} N_e \quad \text{with} \quad N_e = \begin{bmatrix} 0_{n_d \times r_2} \\ I_{r_2 \times r_2} \end{bmatrix} \tag{12}$$

is called recovery matrix and describes the transfer function between the disturbing inputs acting in N_e to the states ($e(t)$, $f_e(t)$). Choosing the weighting matrices in the Riccati equation as

$$Q = I_{(n_d + r_2) \times (n_d + r_2)} + q N_e I_{(n_d + r_2) \times (n_d + r_2)} N_e^T \quad \text{and} \quad R = I_{r_1 \times r_1} \quad ; \quad q \in R^+ \tag{13}$$

where Q is the weighting matrix for the extended system and R the weighting matrix for the measurements, for any given $\epsilon > 0$ a $q^* > 0$ exists, such that for all $q > q^*$ the matrix $(A_e - L C_e)$ is asymptotically stable and

$$||[Is - (A_e - L C_e)]^{-1} N_e||_\infty < \epsilon \,. \tag{14}$$

Choosing $q \to \infty$ yields to $\epsilon \to 0$.[13] In case of fast changing unknown inputs where $\dot{n}(t)$ is large, the parameter q has also to be chosen very large to achieve satisfactory results. In detail, the weighting matrix as designed in Eq. (13) has the form

$$Q = \begin{bmatrix} I_{n_d \times n_d} & 0 \\ 0 & q I_{r_2 \times r_2} \end{bmatrix} \quad ; \quad q \in R^+ \tag{15}$$

and the weighting matrix R is a $r_1 \times r_1$ identity matrix. The Riccati equation (Eq. (11)) is equivalent to the equations given by

$$A P_{11} + P_{11} A^T + N P_{21} + P_{12} N^T + I_{n_d \times n_d} - P_{11} C^T R^{-1} C P_{11} = 0 \tag{16}$$
$$A P_{12} + N P_{22} - P_{11} C^T R^{-1} C P_{12} = 0 \tag{17}$$
$$q I_{r_2 \times r_2} - P_{21} C^T R^{-1} C P_{12} = 0 \,. \tag{18}$$

The observer feedback matrix is denoted by

$$L = \begin{bmatrix} L_1 \\ L_2 \end{bmatrix} = \begin{bmatrix} P_{11} & P_{12} \\ P_{21} & P_{22} \end{bmatrix} \begin{bmatrix} C^T \\ 0 \end{bmatrix} R^{-1} = \begin{bmatrix} P_{11}C^T R^{-1} \\ P_{21}C^T R^{-1} \end{bmatrix} . \quad (19)$$

The matrix L_2 depends on $P_{21} = P_{12}^T$. If assumption (10) holds, the gains $\parallel L_2 \parallel$ increases by increasing q as shown by Eq. (18). To achieve $\epsilon \to 0$, the weighting parameter has to be $q \to \infty$ and in practical applications the parameter should be $q \gg 1$ which yields from

$$q \gg 1 \quad \text{to} \quad \parallel L_2 \parallel \gg \parallel L_1 \parallel . \quad (20)$$

Interpreting Eq. (7), the H_∞ norm of the transfer function $[Is - L_2C(Is - (A - L_1C))^{-1}N]^{-1}$ becomes smaller for larger parameter q ($q \gg 1$, $\parallel L_2 \parallel \gg \parallel L_1 \parallel$). For smaller $f_e(t)$ an bounded $[Is - (A - L_1C)]^{-1}N$ the state estimation error is getting smaller.

3. DESIGN OF A PROPORTIONAL-INTEGRAL-OBSERVER FOR UNCERTAIN SYSTEMS

The design of the feedback matrices as described above is valid only for systems without measurement noise and model uncertainties. In practical applications uncertainties in model and measurement are present. It may be necessary to consider the uncertainties in the design approach. Assume that the system introduced by Eq. (1) has additive unknown inputs $n(t)$, additive measurement noise $d(t)$ and additive model uncertainties $h(t)$

$$\dot{x}(t) = Ax(t) + Bu(t) + Nn(t) + Hh(t) , \quad (21)$$
$$y(t) = Cx(t) + d(t) . \quad (22)$$

The matrix H describes the input of the model uncertainties $h(t)$. The error dynamics becomes

$$\begin{bmatrix} \dot{e}(t) \\ \dot{f}_e(t) \end{bmatrix} = \begin{bmatrix} A - L_1C & N \\ -L_2C & 0 \end{bmatrix} \begin{bmatrix} e(t) \\ f_e(t) \end{bmatrix} + \begin{bmatrix} L_1d(t) - Hh(t) \\ L_2d(t) - \dot{n}(t) \end{bmatrix} . \quad (23)$$

In frequency domain the error dynamics is described by

$$e(s) = -[Is - (A - L_1C)]^{-1}(Hh(s) + L_1d(s) + Nf_e(s)) \quad (24)$$
$$f_e(s) = -[Is - L_2CG(s)N]^{-1}(L_2CG(s)L_1d(s) + L_2CG(s)Hh(s) + L_2d(s) - s\,n(s)) , \quad (25)$$

with $G(s) = (Is - (A - L_1C))^{-1}$. From Eq. (25) it can be seen that four additive parts for the estimation error exist. The last term is the same as for the system without uncertainties. To minimize the transfer function from $\parallel sn(s) \parallel$ to $\parallel f_e(s) \parallel$ described by $[Is - L_2C(Is - (A - L_1C))^{-1}N]^{-1}$ it is necessary to chose $q \gg 1$ if the changes of the unknown input $(\dot{n}(t), sn(s))$ are large. This leads to $\parallel L_2 \parallel \gg \parallel L_1 \parallel$. Unfortunately, in this case, (as $q \gg 1$, $\parallel L_2 \parallel \gg \parallel L_1 \parallel$) the other additive effects will increase, so that the resulting error $f_e(t)$ also increases.

The feedback matrices have to be designed by the LTR method introduced in the previous chapter, but the gain parameter q can not be arbitrary increased as declared. The estimation error depending on the LTR design parameter q is illustrated qualitatively in Fig. 1. The curve $f : \dot{n}(t)$ denotes the error caused by the derivative of the unknown inputs and the curve $f : d(t), h(t)$ denotes the error caused by the uncertainties. There is an optimal value for q where the error is minimal. The optimal parameter q for a minimal error depends on the quality of the model, on the quality of the measurement and on the derivative of the unknown input to be estimated. To estimate fast changing unknown inputs good measurements and good models are necessary for satisfying results.

The introduced PI-Observer can estimate the states as well as unknown inputs acting on a system. To localize an unknown force, parallel observers realizing an observer-bank can be used. If there are n_k different places where an unknown input can occur, there have to be n_k different PI-Observer implementations with N_i, $i = 1...n_k$. One measurement is in the minimum necessary to estimate one unknown force and an additional measurement is necessary to set up a residuum to locate the input. Choosing the residuum $r_i(t) = y_2(t) - \hat{y}_2(t)$, $i = 1...n_k$ where $y_2(t)$ is a measured state and $\hat{y}_2(t)$ the estimated state, an unknown input can be localized by the minimum of the residuum.

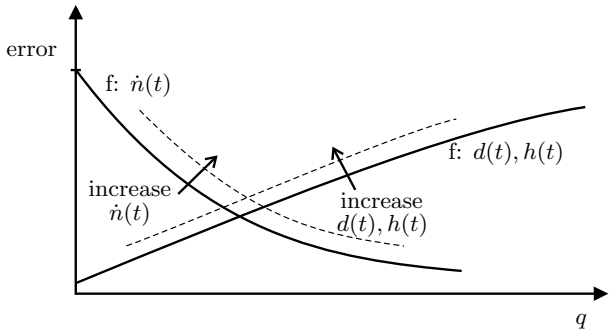

Figure 1. Schematic behavior of the estimation error

4. CONTROL

A state feedback and a disturbance rejection control method is proposed to control vibrations. The PI-Observer is used to estimate the states as well as the unknown inputs (disturbances). The state feedback matrix can be calculated e.g. using the linear quadratic optimal control design approach. The feedback signal is calculated as

$$u(t) \quad = \quad -K_s\hat{x}(t) - K_n\hat{n}(t) + Vw(t) \; , \tag{26}$$

where $K_s\hat{x}(t)$ is the state feedback, $K_n\hat{n}(t)$ is the disturbance rejection term and $Vw(t)$ is the reference signal. The state feedback reduces the oscillations of the modes considered by the model used for the PI-Observer. The disturbance rejection term reduces the effect of disturbances to the parts of a system described by $z(t) = Fx(t)$, where $z(t)$ describes only the part of $x(t)$, on which the effect of a disturbance has to be minimized. The feedback matrix K_n can be calculated as presented in reference[6] by

$$K_n \quad = \quad [F(A - BK_x)^{-1}B] \; F(A - BK_x)^{-1}N \; . \tag{27}$$

If disturbances are considered in the system inputs ($N = B$) the effect of the disturbances can directly be rejected as can be seen from Eq. (1) and Eq. (26). Other works[14,15] deal with alternative approaches realizing dynamic rejection and/or accommodation.

5. MODELING

The PI-Observer can be applied to estimate and locate an unknown force acting on a structure. The method can be used for model-based fault detection and control and can be applied for arbitrary structures, also for 3D structures, if the model of the structure is known (cf. Eq. (1)). Here, a one side clamped elastic beam and an all side clamped elastic plate are used to illustrate the performance of the observer. The introduced method can also be applied to arbitrary 3D structures, if the dynamical model is known.

5.1. One side clamped elastic beam

The one side clamped elastic beam is shown in Fig. 2(a). The scheme of the test rig is presented in Fig. 2(b). An elastic beam clamped on one side gets in contact with the contact surface after a short excursion of the beam (dashed position in Fig. 2(b)). The impact contact force is measured by quartz force sensors, which are mounted between the contact surface and the ground. The displacement of the beam is measured at two points with non-contacting optical measurement systems. There are also 3 strain gages mounted on the beam to measure the strain. This experiment is used to validate and test the PI-Observer for impact forces acting on an elastic mechanical structure. The contact force is estimated using the displacement measurements and (or) the strains. The measurement of the contact force is only used for validation of the observer.

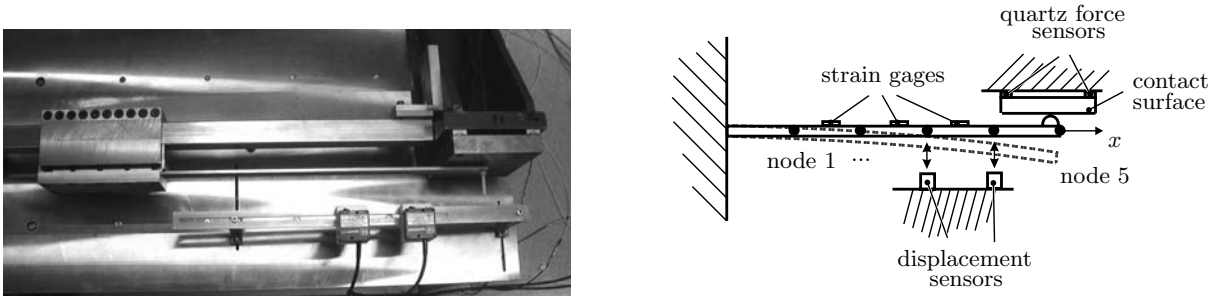

(a) Figure of test rig (SRS, U DuE)

(b) Sketch of the test rig

Figure 2. One side clamped elastic beam

The length of the beam is 548 mm. The beam material is steel and the cross-section area is 30 mm × 5 mm. The strain is measured at position 72 mm, 288 mm and 320 mm. The beam is modeled using five equal finite beam elements. Two displacement measurements are taken in node 3,4 or 5 of the finite element mesh (see Fig. 5.1). The contact point is at the end of the beam and is realized by a steel tip. Additionally, the beam can be excited by a modal hammer which measures the force.

5.2. All side clamped elastic plate

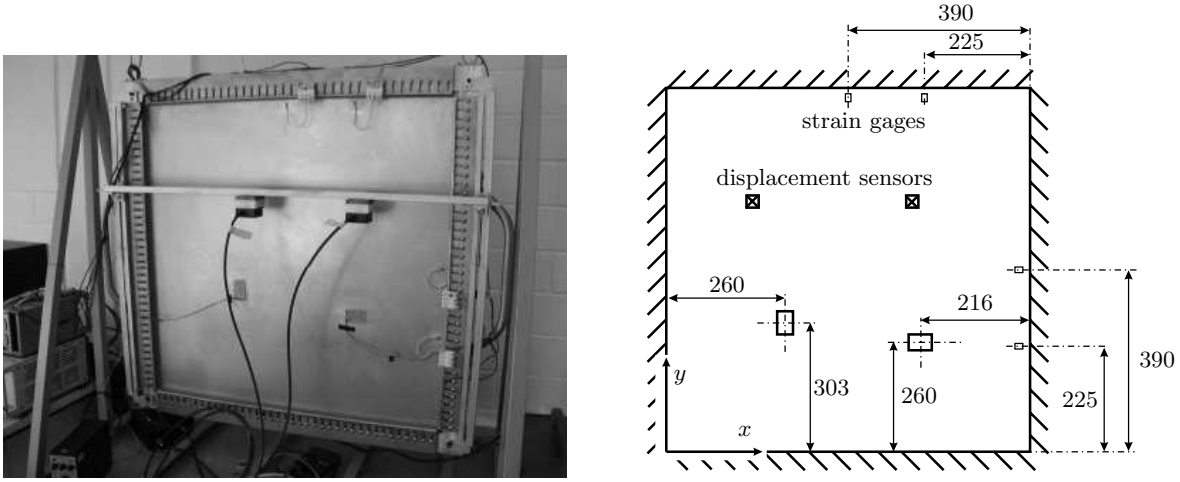

(a) Figure of the test rig (SRS, U DuE)

(b) Sketch of the test rig

Figure 3. All side clamped plate

The experimental setup of the elastic plate is given in Fig. 3 (dimensions in mm). The scheme of the test rig with the positions of the actuators and the sensors is shown in Fig. 3(b). The plate measures 780 × 780 mm and has the thickness $d_p = 0.7$ mm. Two piezo actuators (PZT patches) are bonded on the plate as shown. The displacements are measured at two points with non-contacting optical measurement systems and the strains are measured at the illustrated positions in length direction of the drawn rectangles (see Fig. 3(b)). The plate

is excited by a hammer, which directly measures the contact force. The plate is modeled using 64 equal plate elements (with different boundary conditions). The modeling of the introduced plate is very difficult because of the changing properties of the environment (temperature). The first eigenfrequency of the plate e.g. varies temperature-dependent between 9 Hz to 18 Hz. A connection between the temperature and the eigenfrequency can not be found easily. In the following, these effects are considered by adapting the stiffness matrix to the actual dent of the plate.

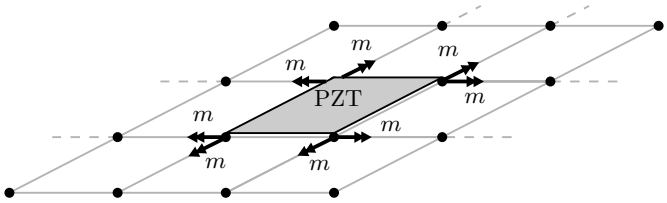

Figure 4. Acting moments from the PZT patch

The moments/forces of the PZT patches acts on the plate structure as shown in Fig. 4. For the control, the plate is divided into 169 equal plate elements. The mesh of the finite elements is chosen such that each corner of the PZT patches is approximately on one finite element node. Applying voltage to the PZT patches they expand and induces forces parallel to the plate surface. In this work, the actuating forces are applied as moments in the nodes as shown in Fig. 4. Many papers deal with the modeling of PZT actuators and the interaction with plate structures.[1] Here, a simple model as given in reference[16] by

$$M_{\mathrm{PZT}} = E_p d_{31} b_p h V \tag{28}$$

is used. The parameters E_p, d_{31}, b_p and h are geometrical and material parameters of the PZT and are constants. The resulting moment M_{PZT} is proportional to the applied voltage V. This is a linear approximation of the actuator behavior. There are numerous works describing the PZT patches in more detail.[1] Here, the simple model given by Eq. (28) is used.

The actuator placement defines the controllability of the structure. To chose appropriate PZT positions a system given by Eq. (1) is considered without unknown inputs ($n(t) = 0$) and transformed by $x(t) = \phi\,\tilde{x}$, where ϕ is the modal matrix of the system. The system is described in modal coordinates by

$$\dot{\tilde{x}}(t) = \tilde{A}\tilde{x}(t) + \tilde{B}u(t)\,, \tag{29}$$

$$y(t) = \tilde{C}\tilde{x}(t)\,. \tag{30}$$

From matrix $\tilde{B} = \phi^{-1}B$ it can be seen if and how strong the modes of the system can be influenced. The same approach is used in reference[17] to place the actuators. From practical point of view only few of the first modes has to be considered. Considering the matrix $\tilde{B}$ for the system given in Fig. 3 with 169 equal finite plate elements, the positions of the PZT patches shown in Fig. 3 are chosen and present a good combination to excite the first 4 modes of the system.

The location of the sensors is also important for the observability of the structure. The strain gages are positioned where the stress is maximal for the first and second mode, in order to get a high resolution for the measurements. The states of the finite element model of the plate contain displacements $w(x,y,t)$ and bendings $(\frac{\partial w(x,y,t)}{\partial x}, \frac{\partial w(x,y,t)}{\partial y}, \frac{\partial^2 w(x,y,t)}{\partial x \partial y})$ of the finite element nodes and their time derivatives. The strain measurement delivers for the x direction $\frac{d_p}{2}\frac{\partial^2 w(x,y,t)}{\partial x^2}$ and $\frac{d_p}{2}\frac{\partial^2 w(x,y,t)}{\partial y^2}$ for the y direction. Another usual method modeling plate structures is the modal analysis.[18] The plate transverse deflection at a point can be described as

$$w(x,y,t) = \sum_{i=1}^{\infty}\sum_{j=1}^{\infty} w_{ij}(x,y) q_{ij}(t)\,, \tag{31}$$

where $w_{ij}(x,y)$ is the plate displacement modal amplitude and $q_{i,j}(t)$ are the generalized coordinates. More detailed descriptions are given in reference.[18] Using

$$\frac{\partial^2 w(x,y,t)}{\partial x^2} = \sum_{i=1}^{\infty}\sum_{j=1}^{\infty}\frac{\partial^2 w_{ij}(x,y)}{\partial x^2}q_{ij}(t)\ , \tag{32}$$

$$\frac{\partial^2 w(x,y,t)}{\partial y^2} = \sum_{i=1}^{\infty}\sum_{j=1}^{\infty}\frac{\partial^2 w_{ij}(x,y)}{\partial y^2}q_{ij}(t) \tag{33}$$

the displacements can be calculated by the strain gage measurements. In this experiment, four strain gage measurements are used (see Fig. 3), so only $w_{11}(x,y)$, $w_{21}(x,y)$, $w_{12}(x,y)$ and $w_{22}(x,y)$ can be considered. For the beam, Eq. (31) has only to be considered for the x direction.

6. EXPERIMENTAL RESULTS

6.1. Contact force estimation for the beam example

The beam gets in contact with the contact surface after a short excursion of the beam (dashed position in Fig. 2(b)). The displacement is measured in node 4 and 5. In Fig. 5(a) and 5(b) the measured and the estimated force are compared. In Fig. 5(a) the design parameter $q = 10^3$ is too small, the observer can not follow the fast dynamic of the contact force. In Fig.5(b) the design parameter $q = 10^8$ is too high, the error caused by the measurement noise and the model uncertainties prevails. Choosing $q = 10^6$ the PI-Observers can estimate the contact force very good as can be seen from Fig. 6(a). The contacts are very fast, up to 5 ms for a contact. In Fig. 6(b) the displacements in node 4 and 5 are calculated by the strain gage measurements. Here, the results are not so good as for the displacement measurement. The calculation from the strain gages to the displacements yields to some differences in the displacement signals which is interpreted as measurement noise. The force can also be estimated for measurements in other nodes and for contacts in other nodes. For slower contacts the estimation results get better.

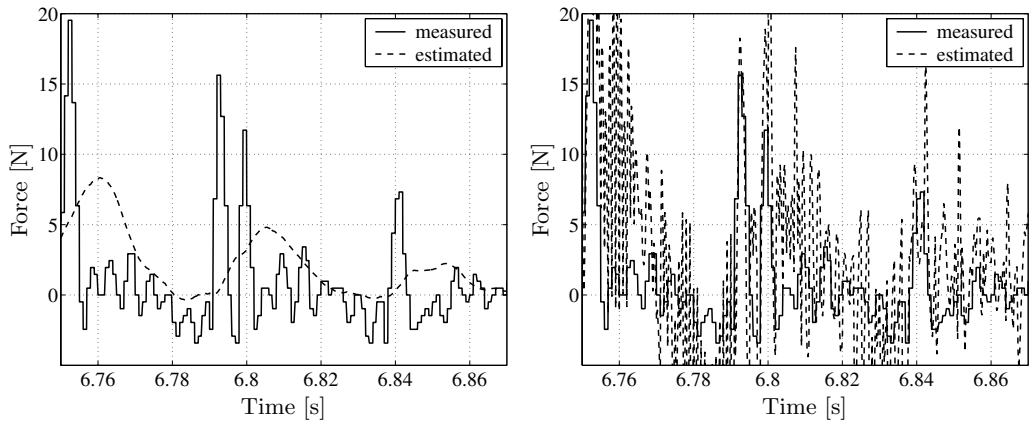

(a) Measurement of displacements in node 4 and 5, $q = 10^3$, too small

(b) Measurement of displacements in node 4 and 5, $q = 10^8$, too high

Figure 5. Contact in node 5

The location is detected using a parallel set of PI-Observers. Every observer needs one measurement to estimate one unknown input. To define the location of the unknown input also only one (additional) measurement is necessary to generate a residuum. In this case, the measurement of the displacement to estimate the unknown

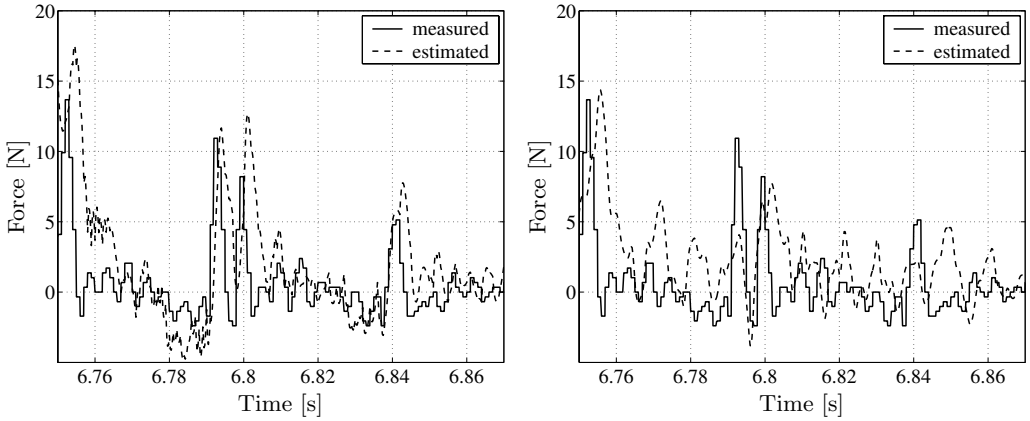

(a) Measurement of displacements in node 4 and 5, $q = 10^6$

(b) Strain gage measurements, $q = 10^6$

Figure 6. Contact in node 5

input is taken in node 3 and the displacement to generate the residuum in node 5. From Fig. 7(a) it can be seen that for the assumed contact in node 1, the residuum has the smallest value. In Fig. 7(b) the result is shown when the contact is in node 3. The first vertical line in the plots denotes the first moment of the contact and the second the maximal amplitude of deflection during the contact.

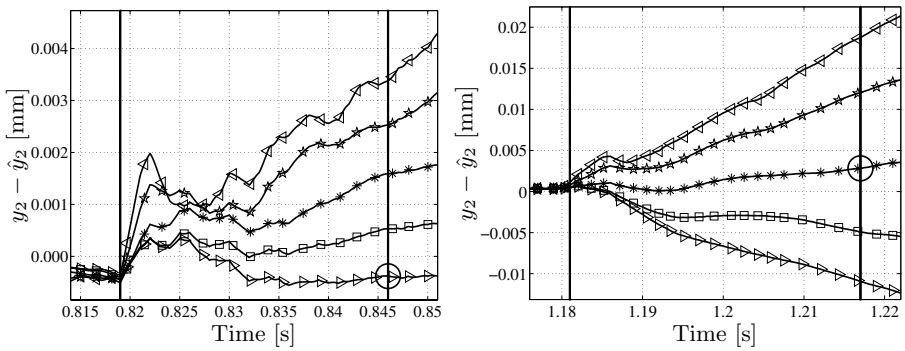

(a) Contact in node 1, displacement measurements

(b) Contact in node 3, displacement measurements

Figure 7. Five parallel PI-Observers with N_i, $i = 1...5$

The results for the strain gage measurements are shown in Fig. 8(a). The displacement of node 3 and 5 are calculated from the strain gage measurements and used in the same way as for the displacement measurements for the localization of the contact. For the strain gage measurements, sometimes it is not possible to distinguish between the contact in node 1 and 2. Using the displacement measurements, the contact in every node can be detected. This only works if one of the measurements is in node 5, to get the entire information about the deformation of the beam.

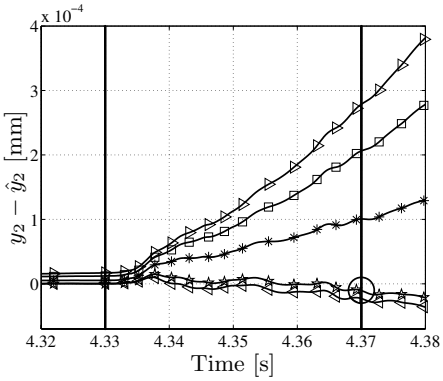

(a) Contact in node 4, strain gage measurements

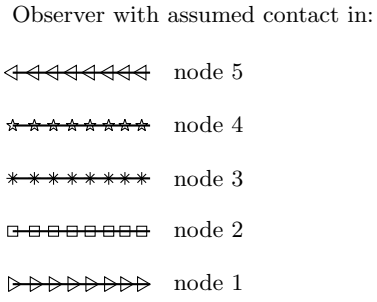

(b) Legend

Figure 8. Five parallel PI-Observers with N_i, $i = 1...5$

6.2. Contact force estimation for the plate example

The displacement measurements for the plate are taken in two different positions. In measurement position 1 the first displacement is measured in ($x = 390$ mm, $y = 585$ mm) and the second in ($x = 585$ mm, $y = 585$ mm, see coordinate system in Fig. 3(b)). The measurements are collocated with the nodes of the finite element mesh. The plate is divided into 64 equal plate elements. In measurement position 2 the first displacement is measured in ($x = 390$ mm, $y = 390$ mm) and the second in ($x = 585$ mm, $y = 390$ mm). A contact in two different positions, contact 1 ($x = 390$ mm, $y = 390$ mm) and contact 2 ($x = 585$ mm, $y = 390$ mm) are applied to the plate.

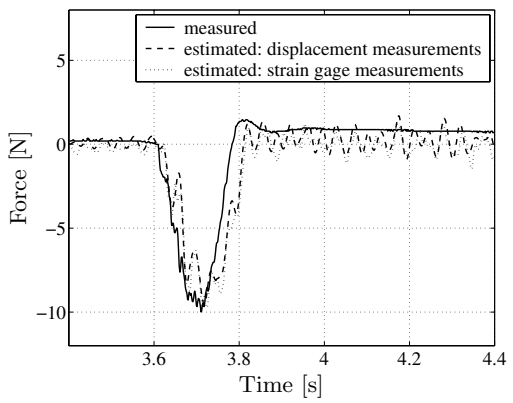

(a) Measurement position 1, contact 1, $q = 10^6$

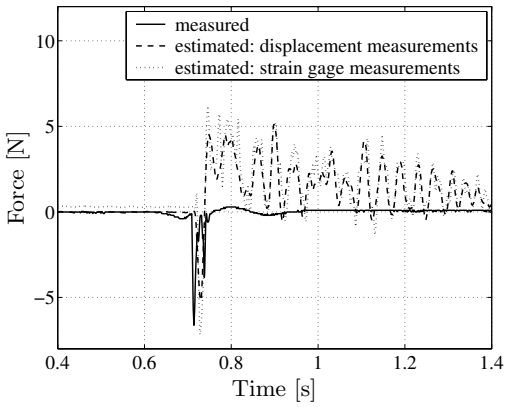

(b) Measurement position 1, contact 1, $q = 10^6$

Figure 9. Estimation of a contact force applied to the plate

In Fig. 9(a) the measured and the estimated contact force are compared. The measurement of displacements is taken in measurement position 1 and the contact is applied in position contact 1. The estimation is done

using the displacement measurement and the strain gage measurement. The contact duration is up to 0.2 s, the estimation is satisfactory. Faster contacts as shown in Fig. 9(b) cannot be estimated satisfactory. The contact can be detected but after the contact the estimated force oscillate with the same amplitude as the contact itself. The model of the plate seems not to be sufficient.

In Fig. 10 the estimation is shown for the displacement measurement in measurement position 2 and the contact is applied in position contact 2. The results are similar as presented before.

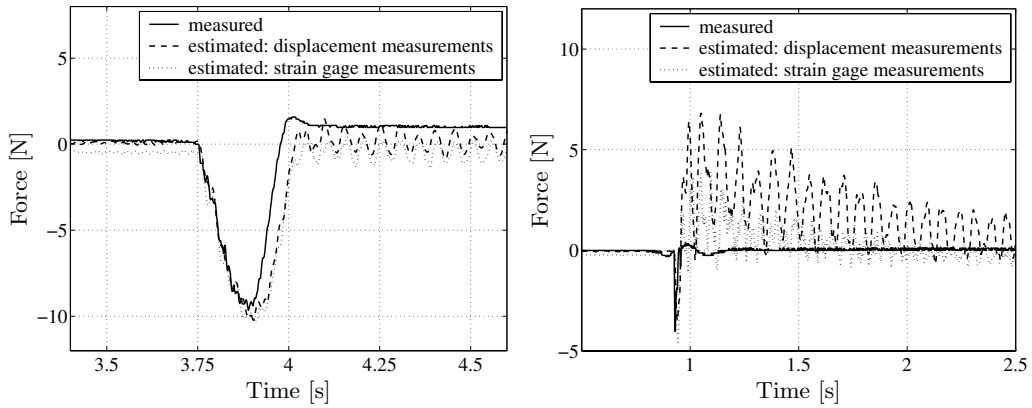

(a) Measurement position 2, contact 2, $q = 10^6$

(b) Measurement position 2, contact 2, $q = 10^6$

Figure 10. Estimation of a contact force applied to the plate

6.3. Control of elastic vibrations of the plate

In Fig. 11 a simulation result of the proposed control approach is shown. Displacements of the plate are measured at two different positions, y_1(x=360 mm,y=540 mm), y_2(x=600 mm,y=540 mm) and the two PZT patches are bonded in positions as shown in Fig. 3(b). The reference signal is chosen to be $w(t) = 150\ V$ ($V = I_{2\times 2}$). The state feedback matrix is calculated via the linear quadratic optimal control design approach. In this case, the parameters of the weighting matrix are chosen in such a way that the actuating signal stays between 100 V and 200 V, so they are not optimized from a theoretical point of view. The disturbance rejection part is not applied in this simulation example, since in the real experiment the PZT patches have not enough power for static deformations and only vibration control is possible. In Fig. 11, the control shows very satisfying results in the simulation.

In Fig. 12 experimental results are shown. The measurement y_1 is transformed using the fourier transformation. Here, for the first experimental realization the disturbance rejection part is not applied to the plate. The PI-Observer is used only to estimate the states for the state feedback. The unknown inputs are assumed as to be present in the inputs of the system (N=B). Therefore, the states can be estimated sufficiently, even if the PZT patch models are linear approximations of the real behavior. The control is tuned to reduce the first two eigenmodes. The results in Fig. 12 shows that the first eigenmode can be reduced significantly. The second eigenmode is however not affected in the same way. The reason is due to the problem of having a plate which tends to dent depending on small temperature fluctuations. The second eigenmode should have one eigenfrequency, instead two eigenfrequencies close together are measured for the system. Tuning the first eigenfrequency of the observer to 15.5 Hz, the first peak of the second eigenmode can be reduced to some extend (see Fig. 12(a)) and tuning it to 15 Hz, the second peak can be reduced (see Fig. 12(b)). Here, the tuning of the first eigenfrequency implies also a change of the second eigenfrequency.

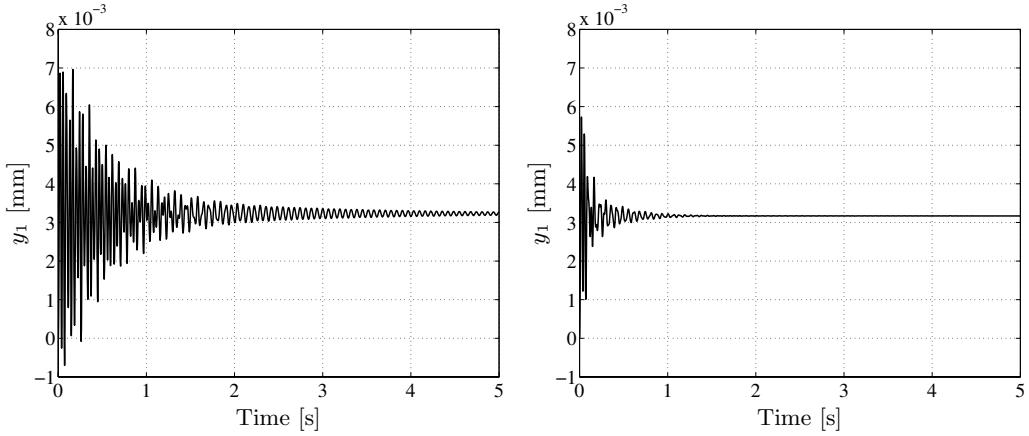

(a) Step response without control

(b) Step response with control

Figure 11. Vibration control of the plate, simulation

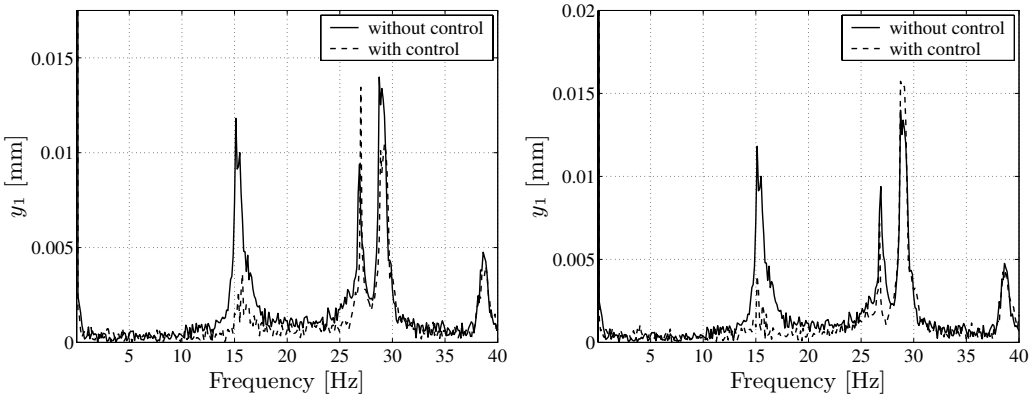

(a) Observer tuned to 15.5 Hz

(b) Observer tuned to 15 Hz

Figure 12. Vibration control of the plate, experiment

7. CONCLUSIONS, OUTLOOK, AND RESTRICTIONS

The analytical design of the PI-Observer is discussed for practical applications, where measurement noise and model uncertainties are present. The performance of the observer is shown for contact force estimation acting upon an elastic beam and an elastic plate. The results for the beam show that, if the model of a system is known, very fast contacts can be estimated sufficiently. Displacement and strain gage measurements are used to estimate the unknown inputs. The location of an unknown input can be detected using parallel observers. Here an additional measurement is necessary to generate a residuum and to estimate the location. The PI-Observer is applied for the first time to a plate structure. It is shown, that the estimation of contacts with a duration time up to 0.2 s works very well and for faster contacts the accuracy of the plate model is not sufficient. The control of the plate structure shows that the first eigenmode can be reduced and the reduction of the second eigenmode depends on the actual dent of the plate and has to be analyzed in more detail. In this case, the applied actuators (PZT patches) have not enough power for disturbance rejection. If more powerful actuators can be used for the

elastic structure, also the introduced disturbance rejection control could be applied. It should be noted that the introduced approach deals with a minimum number of sensors and actuators to estimate dynamic effects and to control vibrations. In future, the approach will be extended and the results will be optimized.

REFERENCES

1. I. Shopra, "Review of State of Art of Smart Structures and Integrated Systems," *AIAA Journal*, Vol. **40**, No. 11, pp. 2145–2187, 2002.
2. P. Pedemonte, W. J. Staszewski, F. Aymerich, M. S. Found, P. Priolo, *Signal Processing for Passive Impact Damage Detection in Composite Structures*, in *Smart Structures and Materials 2001: Modeling, Signal Processing, and Control in Smart Structures*, Vittal. S. Rao, *Proc. SPIE* **2001**, pp. 169–178, 2001.
3. S. J. Kranock, L. D. Peterson, *Real-time structural health monitoring using model-based observers*, *Part of the SPIE Conference on Mathematics and Control in Smart Structures*, San Diego, Californien, USA, pp. 711–722, 1998.
4. I. Krajcin, D. Söffker, *Modified PIO design of robust unknown input estimation*, in *Proc. 19th ASME-DECT Biennial Conference on Mechanical Vibration and Noise, Symposium on Systems with Frictions and Impacts: Modeling, Stability and Control*, Chicago, IL, USA, 6 pages, 2003.
5. P. M. Frank, J. Wünnenberg, *Robust fault diagnosis using unknown input observer scheme*, in *Fault Diagnosis in Dynamic Systems; Theory and Application*, Patton, R.J.; Frank, P.M.; Clark, R.N. (eds.). Prentice Hall, Engelwood Cliffs, 1989.
6. P. C. Müller, *Control of nonlinear systems by applying disturbance rejection control techniques*, *Proc. IEE Int. Conference CONTROL 88*, Institution of Electrical Engineers, London, pp. 734–737, 1988.
7. D. Söffker, *Betriebsüberwachung und Schadensdiagnose an rotierenden Maschine, Bewährte Methoden versus neue modellbasierte Ansätze*, in *Schwingungen in rotierenden Maschinen III*, *SIRM* **95**, Kaiserslautern, Germany, pp. 85–93, 1995.
8. S. O. R. Moheimani, A. J. Fleming, S. Behrens, "Dynamics, Stability, and Control of Multivariable Piezoelectric Shunts," *IEEE/ASME Transactions on Mechatronics,* Vol. **9**, No. 1, pp. 87–99, 2004.
9. J. Tang, K. W. Wang, "Active-passive hybrid piezoelectric networks for vibration control: comparisons and improvement," *Smart Mater. Struct.*, **10**, Institute of Physics Publishing, pp. 794–806, 2001.
10. Vittal S. Rao, S. Sana, *An Overview of Control Design Methods for Smart Structural Systems*, in *Smart Structures and Materials 2001: Modeling, Signal Processing, and Control in Smart Structures*, Vittal. S. Rao, *Proc. SPIE* **2001**, pp. 1–13, 2001.
11. H. H. Niemann, J. Stoustrup, B. Shafai, S. Beale, "LTR design of proportional integral observers," *Int. J. Rob. and Nonl. Control*, Vol. **5**, pp. 671–693, 1995.
12. Y. Xiong, M. Saif, *Output derivative free design of unknown input plus state functional observer*, in *Proc. of the American Control Conference*, Chicago, Illinois USA, pp. 399–403, 2000.
13. J. Doyle, G. Stein, "Robustness with observers," *IEEE Trans. Automatic Control,* Ac-**24**, pp. 607–611, 1979.
14. P. Hippe, Ch. Wurmthaler, *Zustandsregelung, Theoretische Grundlagen und anwendungsorientierte Regelungskonzepte*, Springer Verlag, Berlin, 1985.
15. D. Söffker, *Zur Modellbildung und Regelung längenvariabler, elastischer Roboterarme*, Fortschritt-Berichte VDI Reihe 8, Nr. 584, Dissertation, VDI-Verlag, 1995.
16. A. Preumont, *Vibration Control of Active Structures, An Introduction*, Kluwer Academic Publishers, 1997.
17. U. Gabbert, H. Köppe, F. Seeger, *Overall design of actively controlled smart structures by the finite element method*, in *Smart Structures and Materials 2001: Modeling, Signal Processing, and Control in Smart Structures*, Vittal. S. Rao, *Proc. SPIE* **2001**, pp. 113–122, 2001.
18. L. Meirovitch, *Elements of vibration Analysis*, second edition, McGraw-Hill, 1986.